Adaptive planar vision marker composed of LED arrays for sensing under low visibility

Kyukwang Kim[a], Jieum Hyun[b] and Hyun Myung[*]

Urban Robotics Laboratory(URL), Korea Advanced Institute of Science and Technology,
291 Daehak-ro, Yuseong-gu, Daejeon 34141, Republic of Korea

Abstract. In image processing and robotic applications, two-dimensional (2D) black and white patterned planar markers are widely used. However, these markers are not detectable in low visibility environment and they are not changeable. This research proposes an active and adaptive marker node, which displays 2D marker patterns using light emitting diode (LED) arrays for easier recognition in the foggy or turbid underwater environments. Because each node is made to blink at a different frequency, active LED marker nodes were distinguishable from each other from a long distance without increasing the size of the marker. We expect that the proposed system can be used in various harsh conditions where the conventional marker systems are not applicable because of low visibility issues. The proposed system is still compatible with the conventional marker as the displayed patterns are identical.

Keywords: image processing, marker vision, LED arrays

1. Introduction

Planar vision marker systems that are generally made of printed black and white two-dimensional (2D) patterns have been widely used for various robotic applications including information encoding, image processing, augmented reality (Toyoura *et al.* 2013), and localization (Jung *et al.* 2013). Several marker patterns such as quick response (QR) codes, AprilTags, and ArUco were proposed (Kim *et al.* 2016, Li and Liu 2016). These marker systems are widely used as they can be easily generated, printed, and installed at a low cost and they require low maintenance. They can provide encoded information and the camera pose can be estimated by utilizing appropriate computer vision techniques. Passive markers also have their own benefits—they can be deployed without electricity which is essential in active beacon systems such as Radio Frequency (RF) beacons (Jung *et al.* 2015); however, it is difficult to use the passive marker systems in low visibility environments in which finding the markers in the image is hard or nearly impossible. Robots operating with indoor marker systems can face failure of lightings. Outdoor

∗Corresponding author, Professor, E-mail: hmyung@kaist.ac.kr
[a]M.Sc. Student, E-mail: kkim0214@kaist.ac.kr
[b]M.Sc. Student, E-mail: jimi.hyun@kaist.ac.kr

robots such as drone landing systems (Jung *et al*. 2016) or unmanned underwater vehicles (UUV) that rely on the markers (Han *et al*. 2012) cannot operate at night or at sea with high turbidity.

Active markers have been used to overcome the limitations of the passive markers. Applications that use light emitting diodes (LEDs) as a point indicator or a light communication medium for docking the underwater robots were proposed (Lee *et al*. 2003, Sohn *et al*. 2012); however, these methods require additional specialized hardware modules for LED-based communication, and they lose the merits of the 2D planar markers such as the encoded information or camera position calculation.

In this paper, we propose a planar 2D marker composed of LEDs to overcome the aforementioned problems. The planar vision markers are well-established systems that contain useful information but are not observable in low visibility environments. The LEDs are observable in low visibility environments as they are light sources, but they are not compatible with the conventional marker-based systems. By combining the two systems, we propose a system that exhibits the merits of both systems. A matrix of LEDs is used to display a dot image of n × n markers (n = 8 in this paper). The image is processed to recognize the glowing red lights and converted into a binarized image. Finally, the detected regions are converted into an image with size similar to the printed planar markers. Experiments are designed and performed to show that the LED markers are feasible and that they are compatible with the printed planar marker systems but they can still be operated in low visibility environments where the printed markers cannot be used.

2. Materials and methods

The proposed active marker node comprises an LED matrix for the planar marker display, a distance sensor, and a communication module to detect the proximity of the robot. The functions of the distance sensor and the communication module are described in Sections 2.3 and 2.4, respectively. The 3D-printed casings were designed to hold the display and sensors at appropriate positions. The circuit diagram and an image of the developed node are shown in Fig. 1.
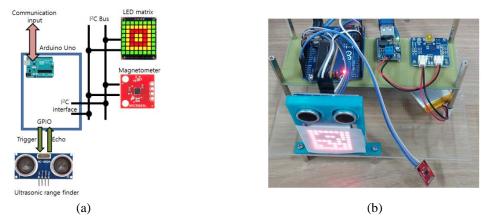

(a)   (b)

Fig. 1 (a) Circuit diagram of an active marker node. GPIO stands for General Purpose Input and Output. The magnetometer and ultrasonic range finder were used for checking the robot proximity and (b) Image of the developed marker node
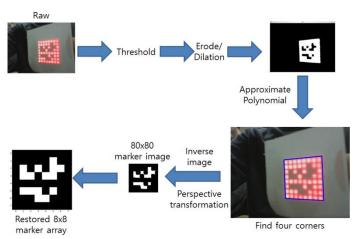
Fig. 2 Overall image processing algorithm for marker detection.

2.1 Image processing algorithms for the LED marker detection

The LED marker is a bright red-colored square LED matrix, which is easily detectable. The acquired raw image was split into RGB channels, and the R channel grayscale image was converted into a binary image by thresholding. Image erosion and dilation were performed to remove the noise from the image. The contours in the image were detected and passed to a polynomial approximation function, and the contour with four corners was selected as a marker. A perspective transformation was used to convert the detected rectangle with an arbitrary shape and size into a square of 80×80 pixels. The square was divided into an 8×8 grid (10×10 pixels per grid), and each grid was color coded as white or black based on the ratio of the black pixels to the white pixels in the grid, reconstructing the final marker image matrix. The developed image processing algorithm is shown in Fig. 2.

2.2 Experiments under the low visibility conditions

The key feature of the proposed marker is its detectability in low visibility environments. There are many low visibility cases such as high smoke concentration in the atmosphere, high turbidity water, or environments where no lightings are available. The active marker node was placed in a completely dark room, and we checked whether the displayed markers could be recognized appropriately. For further examination, a marker detection experiment was conducted under fog generated by a fog machine.

The major application of the printed marker tag is the estimation of the camera pose by calculating the extrinsic/intrinsic parameters of the camera with the real world/image marker coordinates. The proposed marker system was tested for the same task. The marker was assumed to be fixed at the origin (0, 0, 0 in the real world coordinate) with a ruler and protractor for the ground truth measurement. The distance and angle of the camera were calculated by using the solvePnP function of the OpenCV library. The camera was calibrated by a robot operating system (ROS) camera calibration package. The results of the previous experiment showed that a printed marker of size 25×25 cm is visible at a distance of 1.0-1.5 m from the camera. A marker of size 3.2×3.2 cm was used in this research, so the experiments were carried out at a condition of 1/8

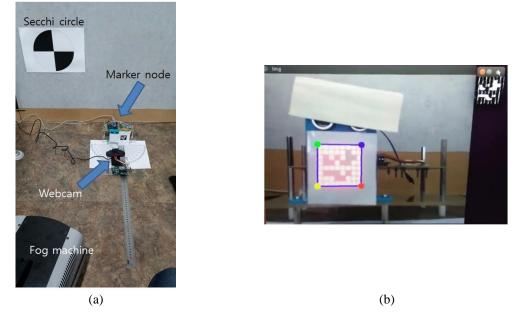(a)   (b)

Fig. 3 (a) Experimental setup. (b) Image acquisition and marker recognition under clear bright situation
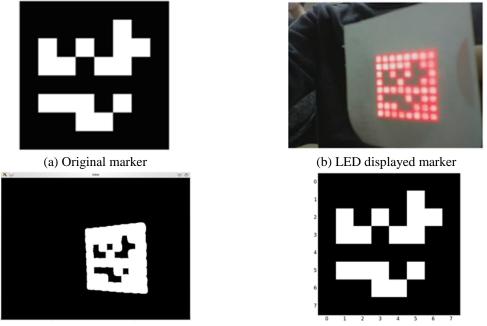
scale (approximately 10 cm) of the conventional setting. The marker and the camera were fixed at the given points (marker at the origin and camera 10 cm away from the marker), and the camera was placed to face the marker directly. Translation and rotation vectors were calculated, and the distance along the x-direction and the yaw angle from the marker were compared with the ground truth (10 cm and 0° meaning front facing). The conventional printed 2D marker with the same pattern was also tested for comparison. The experimental setup is shown in Fig. 3.

The properties of the LEDs were also used for a better identification of the markers. It is rather difficult to generate large-sized markers with the LED matrix compared to the printed markers. Instead, we used the fact that the LED lights can be detected from a long distance even if the size of the display is small. Each LED matrix blinks at its own frequency, so the robots can recognize the small marker from a long distance where the details of the markers are not recognizable. When the robot is close enough to the marker, the details of the marker are recognizable. The distance sensor attached to each active marker system recognizes the nearby object, and the marker stops blinking for easier image processing.

3. Result and discussion

3.1 Reconstruction of LED matrix displayed markers

The results of the marker restoration from the LED image is shown in Fig. 4. The marker detected from the image of the LED matrix (Fig. 4(d)) was identical to the pattern of the original marker (Fig. 4(a)). The result depicted in Fig. 4(c) shows that the binarized image of the LED marker is similar to those of the paper markers. Although the outer form of the shapes of the markers is different, the intermediate results from the image processing operation of the LED

(a) Original marker

(b) LED displayed marker

(c) Image processing

(d) Restored marker

Fig. 4 Restoration of the marker from LED marker. (a) Original AprilTag marker image, (b) LED displayed marker, (c) Contour image of the marker detected during image processing and (d) Restored marker from an inverted contour image, which is identical to the original marker

markers and that of the printed planar markers are identical. This shows the compatibility of the LED markers with the conventional printed planar markers. After simple color filtering and thresholding, previously developed methods and algorithms such as the camera pose estimation, augmented reality, and localization for the printed markers can be directly applied. As mentioned earlier, the markers composed of a few LEDs cannot be used in the mentioned applications because they do not contain many information and adequate corners and areas for the geometric calculation, which is required for the pose estimation.

3.2 Detection under the low visibility environments

The LED marker was placed in a dark room and foggy environment to test the detectability in a low visibility environment. The results are shown in Fig. 5.

Reflection caused by the LED lights can be a source of error. Smooth reflective surfaces such as clean metals that are near the marker can be integrated with the contours. The translucent sheet and the blue 3D printed casing covering the edges of the LED matrix, shown in Figure 1.b, were designed to prevent the formation of an adjacent reflecting point by avoiding the direct attachment of the LED matrix to foreign materials.

The blinking frequency was detected by placing the marker 2 m away from the camera in the dark room. Only one marker was assumed to be at sight. The frame per second (FPS) of the camera stream and the number of the frames in which the majority of the pixels in the selected contour coordinates are white (LEDs turned on) were counted. The ratio of the white frame counts
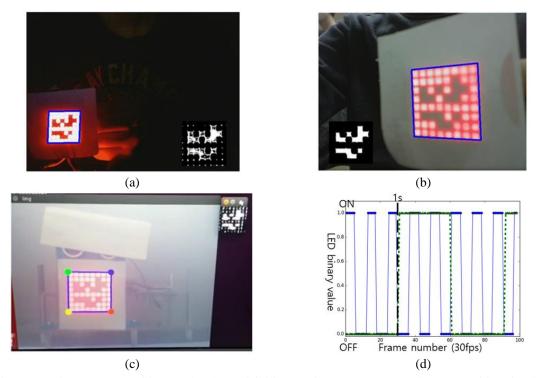
(a)

(b)

(c)

(d)

Fig. 5 Marker ID recognition under low visibility environment. (a) Marker recognition in dark environment. Perspective transformation result is indicated at the right corner, (b) Marker recognition in the normal environment. Perspective transformation result is indicated at the left corner, (c) Marker recognition in foggy environment and (d) Blinking detection plot of 200 ms and 1,000 ms settings. Blue circled line indicates 200 ms blinking while green triangle dashed line shows 1,000 ms blinking. The value of 1 was given when the contour were found at the frame number (30 fps speed). Black long dashed line indicates 1s time interval

Table 1 Distance and angle measurements using LED marker and printed marker

	Ground Truth	LED	Printed
Distance	10 cm	13.06±0.07 cm	12.4±0.04 cm
Angle	0˚	4.89˚±1.06	4.84˚±0.7

to the FPS indicates the period of the blinking LED and the inverse of the period is the frequency. The blinking delays (time that the LEDs are turned on/off) of 1,000 ms and 200 ms (LED turned on for a given time and turned off for the same duration) were tested and the frequency calculator successfully calculated the frequency of the blinking LEDs (average and standard deviation of 229±19 ms in the case of 200 ms blinking and 989±133 ms in the case of 1,000 ms, respectively).

A printed planar marker of approximately 25×25 cm needs to be observed at a similar distance. For the detection of a longer distance, the size of the planar marker has to be gradually increased. However, only an LED matrix of size 4×4 cm can generate similar observability compared to the printed markers. Decreasing the size of the active marker is a great advantage because it requires waterproofing processes, unlike the passive printed markers, and the ease of sealing increases with

the decrease in the size. Decreasing the size can be an advantage in the case of cleaning. Underwater structures suffer from the sea adherences such as seaweeds and barnacles. A smaller size of the marker decreases the area to be cleaned and monitored and the area covered by coatings, preventing these adherences. In addition, a smaller size can help minimize the modification of the original underwater structure on which the marker has to be attached. The pose and the position of the camera were calculated for testing the compatibility of the proposed LED markers with the conventional printed 2D marker systems. The difference in the distance and the angle from the ground truth data was measured and the results are shown in Table 1.

The root mean square errors (RMSEs) of the distance and angle measured by using the LED marker were 3.0 cm and 4.89˚, respectively, whereas the RSMEs of the distance and angle measured by using the printed marker were 2.4 cm and 4.84˚, respectively. The scaled down experiment showed that the proposed marker could be used like the conventional printed markers. Although there were some errors in the distance measurement, a measurement similar to that of the conventional printed markers was obtainable. The measurement made using the LED marker had a slightly higher error than that using the printed markers. The boundary of the recognized LED markers becomes slightly larger than the original marker because the light scattered by the surface of the marker cover is also detected during the thresholding processes. We prospect that this is the cause of the increased error. In addition, the size of the marker used in this research is relatively smaller than that used in the real world applications. Even small errors at the boundary can affect the overall results significantly when compared to the large-sized markers. Because the purpose of this research is to show that the LED markers can function like the conventional 2D markers by using the same algorithms, we did not elaborate further on the accuracy.

The similar experiment was conducted in a foggy environment to compare the printed marker and the LED marker in the same environment. Because the turbidity measurement sensor works only in water, the exact scale of the thickness of fog was not measurable. Instead, the smoke generated by the fog machine (HN-1200W, Hanasound. Inc., Seoul, Republic of Korea) was filled until the Secchi circle with a diameter of 20 cm becomes invisible at a distance of approximately 2 m (about 4 NTU). According to (Jang *et al.* 2015), normal seawaters generally showed 1 to 10 which is similar to the value used in this research. A brown background wall shown in Fig. 3(b) becomes invisible (Fig. 5(c)), indicating the increase in the turbidity. Controlling and maintaining the turbidity of a small gap (10 cm) between the marker and a camera with the fog generated by the fog machine is difficult because the fog tends to rise to the ceiling. Thus, the markers were moved to a distance of 30 cm for the homogenous turbidity between the overall environment and the region between marker and camera, and we checked whether their contour edge is detectable. The proposed marker and the conventional marker exhibited similar functionalities in normal environments. However, the detection ability of the proposed marker and that of the conventional marker differed in a foggy environment. The number of frames at which contours are detected in a foggy environment within the given time was also compared. Among the 327 frames passed, the LED marker detected contours in all the 327 frames. Meanwhile, the contour of the conventional printed marker was detected in only 215 frames (65.7% of success rate). The printed marker was not observable for a few seconds when the fog was belched from the fog machine. However, the light from the LED marker was still observable. In a high turbidity environment, the printed markers are undetectable or they can be wrongly recognized if the grids of the markers are faded. Although the proposed system does not recognize the accurate shape of the marker, it still has a higher visibility and is equipped with the blinking system, which allows long distance detection or high turbidity detection.

4. Conclusions

We have proposed a new active marker system displaying the conventional planar patterned marker with the LED matrix for easier recognition of markers in low visibility environments. The image processing algorithm for the marker restoration and long-range detection by using the blinking frequency were also proposed. Overall experiments showed that the proposed marker is compatible with the conventional printed markers but has higher visibility in various environments.

In the future work, we will consider elaborating the overall system for better detectability and removing errors caused by light reflection and scattering. Also applications of the developed marker at various conditions such as a structural health monitoring (Shin *et al*. 2016), marker based construction assistance (Choi *et al*. 2016, Choi *et al*. 2015), or marker-guided landing of the Unmanned Aerial Vehicles (Jung *et al*. 2015) under low visibility environment will be developed.

Acknowledgements

References

Choi, S., Myeong, W., Jeong, Y. and Myung, H. (2015), "A vision-based 6-DOF displacement measurement method for assemble of PC bridge structures using a planar marker", *Proceedings of the International Conference on Robot Intelligence Technology (RiTA)*, Bucheon, Korea, December.

Choi, S., Myeong, W. and Myung, H. (2016), "A vision-based 6-DOF displacement measurement system using multiple planar markers for precise assemble of PC members", *Proceedings of the International Conference on Control, Automation and Systems (ICCAS)*, Gyeongju, Korea, October.

Han, K., Lee, Y. and Choi, H. (2012), "Vision based framework for autonomous docking of underwater robots using multi-purpose self-similar landmark", *J. CICS*, **4**, 71-72.

Jang, I., Won, D., Baek, W., Shin, C. and Lee, S. (2015), "Turbidity characteristics of Korean port area", *J. Kor. Acad-Industr. Soc*., **16**(12), 8889-8895.

Jung, J., Lee, S. and Myung, H. (2015), "Indoor mobile robot localization and mapping based on ambient magnetic fields and aiding radio sources", *IEEE T. Instrum. Meas*., **64**(7), 1922-1934.

Jung, J., Li, J., Choi, H. and Myung, H. (2017), "Localization of AUVs using visual information of underwater structures and artificial landmarks", *Intel. Serv. Robotics*, **10**(1), 67-76.

Jung, S., Koo, J., Jung, K., Kim, H. and Myung, H. (2016), "Vision-based autonomous landing system of an unmanned aerial vehicle on a moving vehicle", *J. Kor. Robotics Soc.,* **11**(4), 262-269.

Kim, K., Choi, D., Lim, H., Kim, H. and Jeon, J.S. (2016), "Vision marker-based in situ examination of bacterial growth in liquid culture media", *Sensors*, **16**(12), 2179.

Lee, P., Jeon, B. and Kim, S. (2003), "Visual servoing for underwater docking of an autonomous underwater vehicle with one camera", *Proceedings of the OCEANS 2003,* San Diego, California, U.S.A., September.

Li, J. and Liu, H. (2016), "Design optimization of amazon robotics", *Autom. Control Intell. Syst.*, **4**(2), 48-52.

Shin, J., Jeon, H., Choi, S., Kim, Y. and Myung, H. (2016), "Laser pose calibration of visp for precise 6-dof structural displacement monitoring", *Smart Struct. Syst.*, **18**(4), 801-818.

Sohn, K. (2013), "A study on the short-range underwater communication using visible LEDs", *J. Kor. Soc. Marine Eng.*, **37**(4), 425-430.

Toyoura, M., Aruga, H. and Turk, M. (2013), "Detecting markers in blurred and defocused images", *Proceedings of the 2013 International Conference on Cyberworlds (CW 2013)*, Yokohama, Japan, October.

HM